Signal Processing 17 (1989) 191-200
Elsevier Science Publishers B.V.

ITERATIVE RESTORATION OF NOISY ELASTICALLY DISTORTED PERIODIC IMAGES

Michael UNSER[1], Benes L. TRUS[2] and Murray EDEN[1]

[1] *Biomedical Engineering and Instrumentation Branch, Bldg 13, Room 3W13, National Institutes of Health, Bethesda, MD 20892, U.S.A.*

[2] *Division of Computer Research and Technology, National Institutes of Health, Bethesda, MD 20892, U.S.A.*

Received 12 April 1988

Abstract. This paper presents several improvements to an approach that corrects for spatial distortion in quasi-periodic structures in order to achieve noise reduction by averaging. The warping function is represented by quasi-hermite two-dimensional polynomials, a representation that allows great flexibility in the choice of fiduciary points. The estimation of the warping function is refined iteratively. At each iteration, the polynomial coefficients are evaluated from the current position of the reference points; the latter are then relocated by a cross-correlation technique. This procedure is intended to maximize a global signal-to-noise ratio criterion. Experiments with electron micrographs of thin sections of muscle fibers indicate a significant improvement in signal quality when compared with a previous approach. The new method is also shown to be insensitive to the initial position of the reference points.

Zusammenfassung. Der Beitrag beschreibt mehrere Verbesserungsvorschläge für ein Verfahren, das räumliche Verzerrungen in quasiperiodischen Strukturen zu kompensieren und überlagertes Rauschen mit Hilfe einer Mittelwertbildung zu reduzieren gestattet. Die Entzerrungsfunktion wird durch quasi-Hermite'sche zweidimensionale Polynome dargestellt. Diese Darstellungsform gestattet eine hohe Flexibilität in der Wahl der Orientierungspunkte. Die Bestimmung der Entzerrungsfunktion erfolgt iterativ. Bei jeder Iteration werden die Polynomialkoeffizienten aus der aktuellen Position der Referenzpunkte berechnet; letztere werden anschließend durch ein Kreuzkorrelationsverfahren genauer positioniert. Das Verfahren hat das Ziel, global das Signal-Rausch-Verhältnis zu verbessern. Versuche mit Elektronenmikroskopaufnahmen dünner Schnitte aus Muskelfasern ergaben eine signifikante Verbesserung gegenüber dem früher gewählten Ansatz. Das neue Verfahren ist darüberhinaus unempfindlich gegenüber den Anfangslagen der Referenzpunkte.

Résumé. Cet article apporte des améliorations notables à une méthode antérieure permettant la compensation de déformations spatiales pour des structures quasi-périodiques en vue d'une réduction du bruit par cumulation. La fonction de déformation est représentée par une juxtaposition de polynômes bidimensionels permettant une grande flexibilité dans le choix des points de contrôles. L'estimation de la fonction de déformation s'effectue de façon itérative par maximisation d'un rapport signal sur bruit global. Lors de chaque itération, les coefficients polynômiaux sont évalués à partir de la position courante des points de contrôles, ces derniers étant ensuite repositionés par corrélation. Cette nouvelle approche est appliquée à la restoration d'images microscopiques de filaments musculaires et montre une efficacité supérieure. Il apparait également que les performances sont très peu sensibles à la position initiale des points de contrôles.

Keywords. Noise reduction, restoration, periodicity, geometric distortion correction, electron microscopy, image registration.

1. Introduction

It is well known that noisy periodic signals may be enhanced by filtering out their non-periodic components. This operation is implemented either in the Fourier domain by masking out the non-harmonic components of the spectrum, or in real space, by averaging spatially aligned unit cells. This technique is commonly used in the analysis of electron micrographs, particularly in structural investigations of biological macromolecules in ordered arrays [6].

However, even slight departures from exact crystallinity may result in a loss of resolution from the averaged or filtered image, and naturally repetitive structures are often subject to imperfections. These structures may be considered as ideal periodic lattices that have been geometrically distorted. In a previous paper, we have described a computational approach that uses a set of reference points to estimate a spatial warping function represented by separable two-dimensional polynomials [10]. The spatial deformation is then compensated by a geometric transformation. A somewhat related approach has been proposed by Volet et al. for the synthesis of natural structured textures [13].

Although the performance of our previous method was found to be quite promising [7, 8, 10], it suffers from certain limitations. First, its applicability is restricted to cases where the reference points for the undistorted lattice are located at the nodes of a rectangular grid; i.e. their spatial coordinates must be chosen as $(x_{ij}, y_{ij}) = (x_i, x_j)$, where $i = 1, \ldots, n_x$ and $j = 1, \ldots, n_y$. This constraint usually implies that the fiduciary points must be chosen as the four corners of a unit cell, making use of additional points almost impossible. Second, to avoid excessive undulation of the resampling grid, the degree of the polynomials should not exceed five. Therefore, the area of the image to be processed at each step cannot contain a number of unit cells greater than 4×4. Finally, the method is quite sensitive to the initial choice of reference points.

The purpose of this paper is to describe an improved system that overcomes these limitations. First, it allows the choice of an arbitrary number of fiduciary points that can be placed at any spatial location. The estimation of the warping function, which is discussed in Section 2, uses quasi-hermite piecewise polynomials that are known to be computationally stable and quite flexible for interpolation [1]. The dependence on a set of initial parameters is decreased by using an iterative relocation procedure that progressively improves the position of the fiduciary points. This technique is described in Section 3 and the issue of performance evaluation is discussed in Section 4. Finally, the efficacy of the method is illustrated by considering experimental results obtained with micrographs of thin sections of muscle filaments.

2. Unwarping as an interpolation problem

The effect of spatial distortion is described by a one-to-one mapping between the spatial coordinates (x, y) of a gray level value in an ideal coordinate system and its corresponding location $(\tilde{x}, \tilde{y})$ in the distorted lattice. We may therefore conceptualize $\tilde{x}$ and $\tilde{y}$ as bivariate functions of the reference spatial coordinates: $\tilde{x} = f(x, y)$ and $\tilde{y} = g(x, y)$. It is sufficient to consider the sampled values of the horizontal and vertical location functions because our data is discrete:

$$\begin{aligned} \tilde{x}_{k,l} &= f(k\,\Delta x, l\,\Delta y), \\ \tilde{y}_{k,l} &= g(k\,\Delta x, l\,\Delta y), \end{aligned} \tag{1}$$

where Δx and Δy are the horizontal and vertical sampling steps in the x-y plane.

The determination of the warping functions is based on a set of M fiduciary points: $(x_i, y_i) \leftrightarrow (\tilde{x}_i, \tilde{y}_i)$, where $i = 1, \ldots, M$. This set of constraints specifies the value of $f(x, y)$ and $g(x, y)$ at some particular points in the x-y plane. It follows that the extrapolation of the warping functions over the entire plane is in essence an interpolation problem which can be approached in different ways. The essential difficulty is that the values of the functions are known for irregularly distributed data points and that conventional sampling theory is therefore not applicable. In addition, we would like the mapping between both coordinate systems to be as smooth as possible in order to provide a good approximation of an elastic or "rubber-band-type" deformation.

The bivariate interpolation method for irregularly distributed data points due to Akima is particularly well suited to this problem as it represents surfaces by piecewise polynomials which are continuous in their first-order derivatives

[1]. In this approach, which we are applying to the determination of both $f(x, y)$ and $g(x, y)$, the reference points are used to divide the x-y plane into triangular regions. Within each triangle, the interpolating function is a two-dimensional polynomial which is entirely determined from the values of the function and its first- and second-order derivatives at the vertices of the triangle.

2.1. Triangulation

An optimal triangulation requires that any point within a triangle is closer to the triangle's vertices than to vertices of any other triangle. One approach for its determination uses an iterative application of the max-min angle criterion [4]: when a set of four points are vertices of a quadrilateral with no internal angle greater than π, one chooses the triangulation that maximizes the minimum interior angle of the two obtained triangles. More recently, Green and Sibson have proposed a more efficient algorithm based on the Dirichlet tesselation of the set of points [3]. Dirichlet tesselation defines a region for each point of the set with the property that the points within this region are closer to the specified point than to any other set point. Triangulation is then obtained by joining neighbors of the Dirichlet tesselation.

2.2. Piecewise polynomials

The x-y coordinates of the reference points define the vertices of triangular cells that divide the x-y plane. For each of these vertices, the value of the horizontal or vertical location function (e.g. $f(x, y)$ or $g(x, y)$) is known and its first-order and second-order partial derivatives ($\partial f/\partial x$, $\partial f/\partial y$, $\partial^2 f/\partial x^2$, $\partial^2 f/\partial y^2$, $\partial^2 f/\partial x \partial y$) are estimated locally by determining tangent planes to the surface and to its derivative based on the function values at neighboring points. In addition to these constraints, the partial derivatives in the direction perpendicular to each side of a triangle are required to be polynomials of degree three, at most, which guarantees continuity of the interpolating function and its first-order derivatives on each side of the triangle. For each triangle, the value of the function is then interpolated by a bivariate fifth-degree polynomial:

$$f(x, y) = \sum_{p=0}^{5} \sum_{q=0}^{5-p} a_{pq} x^p y^q, \tag{2}$$

whose coefficients are uniquely defined by a set of 21 constraints. The surface obtained by using this approach is smooth in the sense that the interpolating function and its first-order partial derivatives are continuous. An implementation of this algorithm is presented in Algorithm 526 of the ACM [1].

2.3. Spatial unwarping

Once the polynomial coefficients are found, the two-dimensional arrays $\{\tilde{x}_{k,l}\}$ and $\{\tilde{y}_{k,l}\}$ are determined over the whole area of interest from (1) and (2). Unwarping is then achieved by appropriately resampling the original data. Let $\{w_{k,l}\}$ denote the discrete preprocessed image to be unwarped and $\{w(\tilde{x}, \tilde{y})\}$ its corresponding continuous representation. The unwarped image $\{u_{k,l}; k = 1, \ldots, K'$ and $l = 1, \ldots, L'\}$ is computed as

$$u_{k,l} = u(k\Delta x, l\Delta y) = w(\tilde{x}_{k,l}, \tilde{y}_{k,l}), \tag{3}$$

where $w(\tilde{x}, \tilde{y})$ is determined by interpolating $\{w_{k,l}\}$. Usually, it is sufficient to use bilinear interpolation which evaluates $w(\tilde{x}, \tilde{y})$ in terms of its four closest sampled values.

3. Iterative refinement of fiduciary points

In our initial method, the estimation of the coordinates of reference points used a standard cross-correlation technique [10]. Reference templates are usually constructed from a model of the structure being investigated, and the positions of the fiduciary points are determined from the maxima of the corresponding cross-correlation function. The major shortcoming of this technique is that the template is not corrected for spatial deformation and that the detected fiduciary points are therefore not always localized very precisely.

To overcome this limitation, we have developed a procedure by which the position of these points is refined iteratively. A cycle k of this algorithm is described by the following succession of operations:

(a) *Unwarping.* Based on the current set of fiduciary points $\{(\tilde{x}_i^{(k)}, \tilde{y}_i^{(k)}),\ i=1,\ldots,M\}$, the structure of interest is unwarped according to the procedure described in Section 2.

(b) *Cross-correlation.* The positions of all fiduciary points are re-determined by searching for the closest maximum of the cross-correlation of the lattice image with the corresponding reference template. This computation is performed on the geometrically corrected structure in close proximity (typically within 3 pixels in each direction) of each reference position (x_i, y_i) and yields a set of displacement vectors $\{(\Delta x_i^{(k)}, \Delta y_i^{(k)}),\ i=1,\ldots,M\}$. These quantities are determined with sub-pixel accuracy by locally fitting a two-dimensional second-degree polynomial to the computed correlation values and solving for the maximum of this function.

(c) *Updating.* The positions of the fiduciary points are then mapped back into the initial coordinate system according to the equation:

$$\begin{aligned}\tilde{x}_i^{(k+1)} &= \tilde{x}_i^{(k)} \\ &\quad + \alpha(f(x_i+\Delta x_i^{(k)}, y_i+\Delta y_i^{(k)}) - \tilde{x}_i^{(k)}), \\ \tilde{y}_i^{(k+1)} &= \tilde{y}_i^{(k)} \\ &\quad + \alpha(g(x_i+\Delta x_i^{(k)}, y_i+\Delta y_i^{(k)}) - \tilde{y}_i^{(k)}),\end{aligned} \tag{4}$$

where $f(x, y)$ and $g(x, y)$ denote the current estimates of the mapping functions between the distorted and the normalized coordinate systems. The procedure is iterated until the end condition: $[(\Delta x_i^{(k)})^2 + (\Delta y_i^{(k)})^2] < \varepsilon^2$, is met for all $i=1,\ldots,M$.

The constant α in (4) is a damping factor which is usually assigned a value slightly below 1. When $\alpha = 1$, this set of equations puts into correspondence $(\tilde{x}_i^{(k+1)}, \tilde{y}_i^{(k+1)})$ and the current estimate of the position of the reference point on the unwarped lattice: $(x_i+\Delta x_i^{(k)}, y_i+\Delta y_i^{(k)})$. At the next cycle of iteration, the warping functions are recomputed by using the correspondence between $(\tilde{x}_i^{(k+1)}, \tilde{y}_i^{(k+1)})$ and (x_i, y_i) which should have the effect of better repositioning the fiduciary point. Note that the choice of the displacement vectors $(\Delta x_i^{(k)}, \Delta y_i^{(k)})$ that maximize the cross-correlation function tends to minimize the mean square error between the correctly positioned reference template and the unwarped structure. This property can be demonstrated in the particular case in which the resulting incremental geometric correction can be locally approximated by a simple translation.

4. Noise reduction and performance assessment

After compensation of the spatial deformation, the periodicity of the signal in the two principal directions are K and L, respectively. The individual unit cells $\{v_{k,l}^{(i)}\}$, where $i=1,\ldots,N$, are extracted from the unwarped signal as

$$\begin{aligned}&v_{k,l}^{(i)} = u_{k-k_i, l-l_i}, \\ &(k=1,\ldots,K,\ l=1,\ldots,L,\ i=1,\ldots,N),\end{aligned} \tag{5}$$

where (k_i, l_i) is the spatial index of the upper left corner of unit cell i. The average of these unit cells

$$\bar{v}_{k,l} = \frac{1}{N}\sum_{i=1}^{N} v_{k,l}^{(i)}, \tag{6}$$

provides an estimate of the underlying signal while the variance of the noise is reduced by a factor N. The efficacy of this restoration is assessed by estimating the signal-to-noise ratio on the rectified lattice:

$$\mathrm{SNR} = \hat{\sigma}_s^2 / \hat{\sigma}_n^2, \tag{7}$$

where $\hat{\sigma}_s^2$ is an estimate of the signal mean energy

$$\hat{\sigma}_s^2 = \frac{1}{KL}\sum_{k=1}^{K}\sum_{l=1}^{L}(\bar{v}_{k,l})^2, \tag{8}$$

and $\hat{\sigma}_n^2$ an estimate of the noise variance

$$\hat{\sigma}_n^2 = \frac{1}{N-1}\sum_{i=1}^{N}\sum_{k=1}^{K}\sum_{l=1}^{L}\frac{(v_{k,l}^{(i)} - \bar{v}_{k,l})^2}{KL}. \tag{9}$$

The SNR measures the proportion of signal energy that is truly periodic and is therefore a direct measure of the success of our rectification technique. Since our iterative algorithm tends to

minimize the mean square difference between the registered signal and the reference template, it will also tend to minimize the residual noise variance provided that the reference templates used for cross-correlation and the underlying signal are sufficiently similar. Alternatively, we may also choose to recompute our reference templates at each iteration based on the current averaged signal.

An important characteristic of the restored signal is its spatial resolution which can be assessed quantitatively by means of the spectral signal-to-noise ratio (SSNR) criterion [11]. The evaluation of the SSNR is similar to that of the global SNR given by (7)-(9). The essential difference is that the signals are replaced by their discrete Fourier transforms and that spatial summation is replaced by a series of summations over concentric annuli in Fourier space corresponding to increasing radial frequencies.

5. Experimental results

This restoration technique has been applied to the analysis of electron micrographs showing the lattice structure of the "thick", myosin-containing filaments and the "thin", actin-containing filaments in skeletal muscle [7, 8]. These images, which are similar to those used in our previous study, were obtained from cryosections of specimens preserved by rapid freezing in vitreous ice [5].

The data was acquired on a Phillips EM400 electron microscope at a magnification of 15 200×, using low-dose techniques, and scanned with a Perkin-Elmer 1010MG to give an effective sampling step of 1.25 nm.

5.1. Comparative evaluation

A first series of experiments was conducted to compare the performance of our previous method [10] with the new algorithm. The initial extraction of the reference points was performed by an operator and was based on the detection of the maxima of the cross-correlation functions of the original micrographs and two rescaled templates corresponding to the myosin- and actin-containing filaments. These templates were generated by pre-multiplying a reference 44×76 hexagonal unit cell with two circular symmetric Gaussian windows ($\sigma_1 = 12.5$, $\sigma_2 = 7.5$) centered on the thick and thin filaments, respectively. The reference unit cell was obtained based on the data available from previous analyses [7, 8]. The unwarping functions were designed to map an originally hexagonal lattice into an ideal square lattice with 44×44 pixels per unit cell.

With our original unwarping method, the results of which are shown in Fig. 1, the choice of the reference points was restricted to the thick filament centers. The original micrograph is displayed in Fig. 1(a). The unwarping function, which corresponds to the superimposed grid, is modelled by two-dimensional separable polynomials of degree three whose coefficients are determined from the initial position of 16 reference points. The results of the unwarping of this area of 3×3 unit cells is displayed in Fig. 1(b). This image was further decomposed into its residual noise and periodic components, as shown in Figs. 1(c) and 1(d). The extracted signal, $\{\bar{v}_{k,l}\}$, was finally reconverted into a hexagonal lattice and is displayed in Fig. 1(e) as the final rescaled result of processing. The signal-to-noise ratio as computed by (7)-(9) on the square lattice is 0.608.

Since the new algorithm puts no constraints on the position of the fiduciary points, we used the centers of both actin- and myosin-containing filaments. An initial unwarping function was computed using the procedure outlined in Section 2 with a total of 34 fiduciary points for this particular example. The polynomials were extrapolated in a 15 pixel wide area surrounding the extracted unit cells to facilitate the relocation of border points. Both reference templates were mapped onto the rectified square lattice and cross-correlated with the geometrically compensated structure to refine the position of all reference points iteratively. Δx and Δy were clipped to a maximum of 3 sampling intervals in each direction and the damping factor in (4) was set to: $\alpha = 1$. The procedure converged

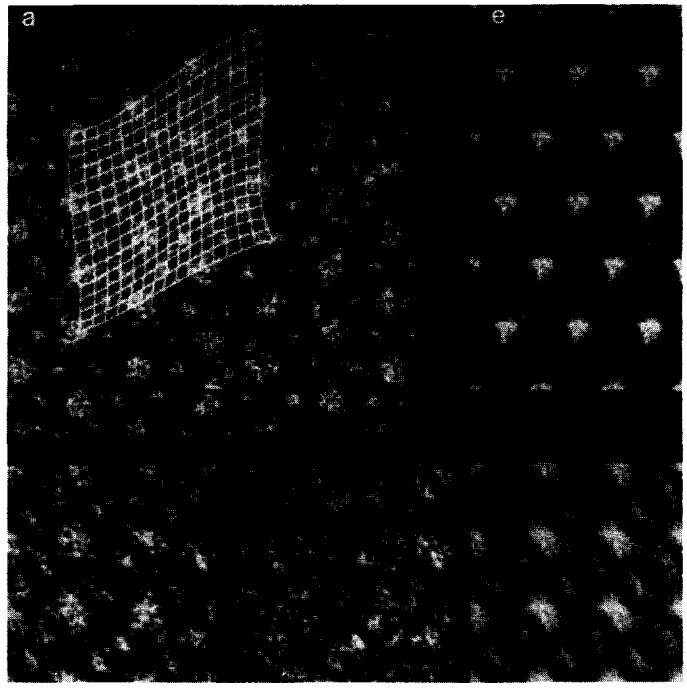

Fig. 1. Processing results obtained with the previous approach. (a) Preprocessed micrograph with superimposed sampling grid. (b) Unwarped unit cells with 44×44 pixels per cell. (c) Stochastic component with $\hat{\sigma}_n^2 = 524.7$. (d) Periodic component with $\hat{\sigma}_s^2 = 319.2$. (e) Periodic component displayed in a hexagonal lattice with fully adjusted dynamic range.

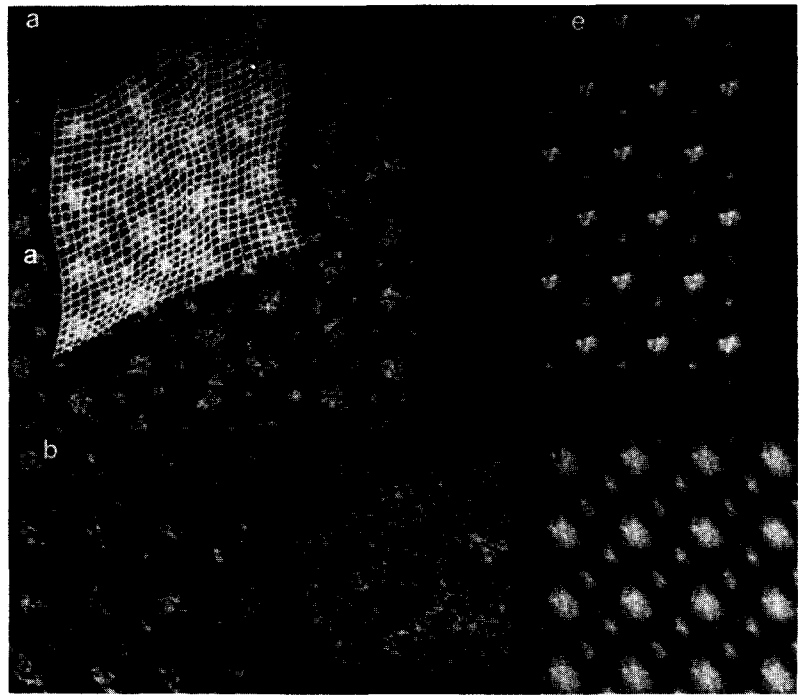

Fig. 2. Processing results obtained with the new approach. (a) Preprocessed micrograph with superimposed sampling grid. (b) Unwarped unit cells with 44×44 pixels per cell. (c) Stochastic component with $\hat{\sigma}_n^2 = 390.5$. (d) Periodic component with $\hat{\sigma}_s^2 = 333.6$. (e) Periodic component displayed in a hexagonal lattice with fully adjusted dynamic range.

in 1 iteration and the final sampling grid is represented in Fig. 2(a). The results of unwarping as well as the decomposition in stochastic and periodic signal components are displayed in Figs. 2(b)-(d). The final result of the analysis, which has been mapped back into a hexagonal lattice, is shown in Fig. 2(e). The measured signal-to-noise ratio is 0.856, which is an improvement of more than 30% over the previous approach.

A visual comparison between Fig. 1(e) and Fig. 2(e) suggests the second method produces a sharper image. This observation is confirmed quantitatively by the analysis of the SSNR[1] curves in Fig. 3. In this example, the SSNR due to the second method is always above that of the first one, which is a strong indication of improved spatial resolution [11]. An operational value of spatial resolution is usually obtained from the cut off point where the SSNR falls below an acceptable limit

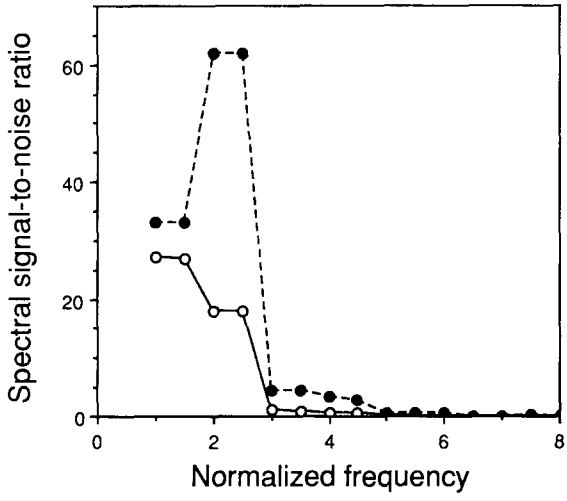

Fig. 3. Spectral signal-to-noise ratio curve as a function of the normalized spatial radial frequency. ○: averaged hexagonal unit cell in Fig. 1(e); ●: averaged hexagonal unit cell in Fig. 2(e).

[1] The spectral signal-to-noise ratio (SSNR) is measured using 44×76 rectangular images (Δx, $\Delta y = 0.85$ nm), each containing a single hexagonal unit cell, which is repeated periodically to fill the available space. This quantity has been multiplied by N (the number of images) since it is associated to the average image. For comparison, the global signal-to-noise ratios of the corresponding averages obtained using both methods are SNR = 6.876 and SNR = 9.99, respectively.

of 4, which in the present case occurs at $f_4 = 1/12.8\ \text{nm}^{-1}$ and $f_4 = 1/10.2\ \text{nm}^{-1}$, respectively. Note that these resolution values are very likely to improve when the number of individual unit cells included in the global average is increased.

5.2. Convergence study

To test the robustness of the iterative relocation procedure, the initial reference points were randomly displaced according to the equation:

$$\tilde{x}_i^{(0)} = \tilde{x}_i + \Delta\tilde{x},$$
$$\tilde{y}_i^{(0)} = \tilde{y}_i + \Delta\tilde{y}, \tag{10}$$

where $\Delta\tilde{x}$ and $\Delta\tilde{y}$ are Gaussian random variables with a zero mean and an adjustable standard deviation σ. Under these conditions, the behavior of the algorithm with the same parameters as in the previous experiment is shown in Fig. 4. These curves represent the signal-to-noise as a function of the number of iterations for different values of σ. When σ is less than 3 pixels, convergence occurs after 1 or 2 iterations. Beyond this point, there is a slight residual oscillation because our determination of the displacement vectors $(\Delta x_i^{(k)}, \Delta y_i^{(k)})$ with

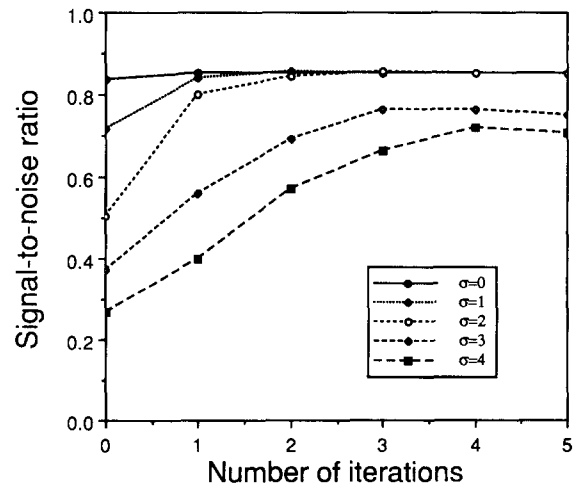

Fig. 4. Signal-to-noise ratio as a function of the number of iterations for various standard deviation of the initial displacement errors (σ). Updating parameters: $\alpha = 1$ and $\Delta x_i^{(k)}$, $\Delta y_i^{(k)} \leq 3$.

subpixel accuracy is only approximate. These oscillations can be suppressed by decreasing α, which in turn will reduce the rate of convergence slightly. When σ is greater or equal to 3, the algorithm seems to be trapped in a local optimum and is not capable of correctly placing some of the reference points. This effect is attributable to the fact that, in the current setting, the search in the determination of $\Delta x_i^{(k)}$ and $\Delta y_i^{(k)}$ is only performed over a distance of 3 pixels in each direction. The performance, however, is still better than that of the first method in the previous section.

In order to be capable of better handling larger displacements, it is appropriate to increase the neighborhood in which the cross-correlation is evaluated. Accordingly, we chose to set the searching distance to twice the value of the standard deviation σ. This led to a significant performance improvement as illustrated in Fig. 5. With this adjustment, the performance of the algorithm only breaks down when $\sigma \geq 5$, an extreme situation in which the initial error for the positioning of some reference points is more than 30% of the distance to the next reference point.

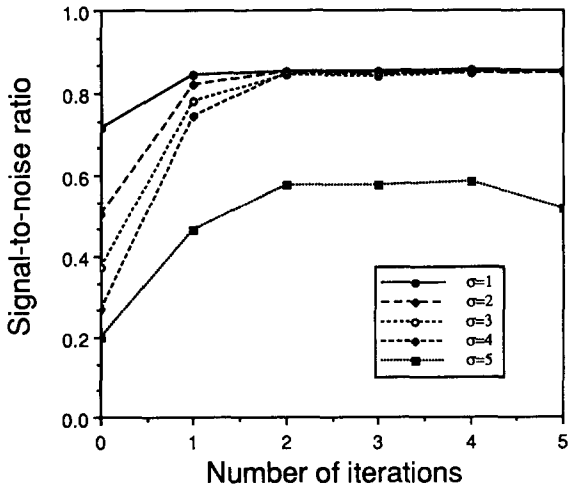

Fig. 5. Signal-to-noise ratio as a function of the number of iterations for various standard deviation of the initial displacement errors (σ). Updating parameters: $\alpha = 1$ and $\Delta x_i^{(k)}$, $\Delta y_i^{(k)} \leq 2\sigma$.

5.3. Discussion

On this example and on all other micrographs that we have analyzed, the new method was always found to be superior to earlier ones. In most cases, the improvement in both SNR and spatial resolution is essentially due to the inclusion of a larger number of fiduciary points. Compensation for the disorderly myofilaments is alway better as can be seen by comparing the amount of structural information that is still present in the so-called stochastic components in Figs. 1(c) and 2(c). For the example discussed in Section 5.1 in which the initial positions of the fiduciary points were quite accurate, the improvement of the SSNR due to iteration was only marginal (e.g. from SNR = 0.838 to SNR = 0.856). However, in other less ideal cases, this feature of the algorithm turns out to be quite important, as was demonstrated in Section 5.2. Another advantage of the present scheme is that it places no contraints on the spatial organization of the unit cells to be processed. These need not be organized in rectangular or trapezoidal patches, as was necessary for the previous method, nor are the cells required to be connected to each another.

In Section 4, we introduced the SNR as an objective performance criterion. Its estimation is essential for it allows us to monitor the progress of the iterative algorithm which can be interpreted as an optimization procedure. For our test experiments, the convergence of the algorithm was found to be very good up to a certain level of misplacement of the fiduciary points. This type of behavior, however, is not guaranteed, as it is strongly data dependent. Fortunately, a lack of convergence or a lack of periodicity is easily detected from the value of the SNR. Following data extraction, it is also advisable to identify non-consistent unit cells, for example, by using some outlier detection scheme such as the OMO algorithm [9], omitting the outliers from the final average.

Our procedure relies heavily on the use of reference templates to locate the position of reference points. Fortunately, the exact shape of the masks is not overly important as they are only used for

signal registration. What is required is that they provide a better match at the exact location of the fiduciary point than in the neighborhood of this point. Typically, the templates are created from an initial approximation of the reference unit cell which can be obtained as follows. The first time a new type of image is analyzed, the fiduciary points are determined first. These unrefined points are used to create what we call an "internal" reference. After refinement converges and unit cells are created, the best cells are averaged after removal of outliers. The average cell is then used as an "external" reference for subsequent refinement of additional images. When working with several data sets, we have found that using an "internal" reference is usually satisfactory. However, whenever possible, it is preferable to use a single fixed "external" template, primarily because it guarantees that the data is globally registered.

In our experiments, we have used a damping factor $\alpha = 1$, which provides the fastest rate of convergence. Such a high value of α may occasionally produce oscillations, particularly when the signal-to-noise ratio is very low. These problems can usually be avoided by using a smaller damping factor, such as $\alpha = 0.7$, which will slightly increase the number of required iterations.

While the technique presented here has been applied to myofilament thin sections, there are obvious potentialities for the restoration of any deformed lattice structures. The piecewise polynomial model of spatial distortion presupposes that the lattice has been deformed in a smooth and continuous fashion. In particular, these assumptions seem appropriate when spatial deformations are due to expansion, compression, or bending of a uniform structure, but not buckling, tearing and the like.

Finally, the first part of the method described in Sections 2 and 3 is also applicable to image registration which is the process of overlaying two images of the same scene or object. Image registration is particularly relevant in remote sensing [12], as well as in medical imaging where it is of interest to map several PET, CT or MRI images onto a common atlas to allow the comparison of measurements obtained from different patients [2].

6. Conclusions

We have presented two improvements to a method that compensates for spatial distortions in quasi-periodic structures and allows efficient noise reduction by cumulative averaging or periodic filtering. The first concerns the modelling of the warping function by piecewise polynomials defined over elementary triangular regions and continuous up to their first order derivatives. The coefficients of these polynomials are determined locally from a set of reference points that can be placed at arbitrary spatial locations. The second improvement is an iterative procedure that progressively re-adjusts the spatial coordinates of the reference points and substantially decreases performance dependence on their initial position.

The main advantage of this new approach over the previous one is that it allows the use of a larger number of reference points per unit cell which greatly improves image restoration, as shown in our experimental examples. Finally, the method has been found to be very robust in the sense that it is tolerant of fairly large errors in the initial positioning of the fiduciary points (up to 1/3 of the distance to the next closest point).

This improved method enables a significant restoration of high resolution micrographs of crystalline or quasi-periodic structures such as found in muscle fibers, and should therefore provide a useful tool for the structural investigation of organized biological systems.

Acknowledgments

We thank Dr. A.C. Steven for helpful discussions, and Drs. R.J. Podolsky, A.C. Steven, A.W. McDowall and J. Dubochet for making available the electron micrographs.

References

[1] H. Akima, "A method of bivariate interpolation and smooth surface fitting for irregularly distributed data points", *ACM Trans. Math. Software 4*, Vol. 2, 1978, pp. 148-159.

[2] R. Bajscy, R. Lieberson and M. Reivich, "A computerized system for the elastic matching of deformed radiographic images to idealized atlas images", *J. Comput. Tomography*, Vol. 7, No. 4, pp. 618-625.

[3] P.J. Green and R. Sibson, "Computing Dirichlet tessellations in the plane", *Comput. J.*, Vol. 21, 1978, pp. 168-173.

[4] C.L. Lawson, "Software for C^1 surface interpolation", in: J.R. Rice, ed., *Mathematical Software III*, Academic Press, London, 1977, pp. 161-194.

[5] A.W. McDowall, W. Hofmann, J. Lepault, M. Adrian and J. Dubochet, "Cryoelectron microscopy of vitrified insect flight muscle", *J. Mol. Biol.*, Vol. 178, 1984, pp. 105-111.

[6] W.O. Saxton, *Computer Techniques for Image Processing in Electron Microscopy*, Academic Press, London, 1978.

[7] A.C. Steven, B.L. Trus, M. Unser, A.W. McDowall, J. Dubochet and R.J. Podolsky, "Myofilament lattice of vertebrate skeletal muscle visualized by correlation averaging of frozen hydrated thin sections", in: G.W. Bailey, ed., *Proc. 44th Annual Meeting of the Electron Microscopy Society of America*, San Francisco Press, August 1986, pp. 108-109.

[8] B.L. Trus, A.C. Steven, M. Unser, A.W. McDowall, J. Dubochet and R.J. Podolsky, "Correlation averaging techniques to rectify disordered myofilament lattices visualized in frozen hydrated thin sections of vertebrate muscle", *XIth Int. Cong. on Electron Microscopy*, Aug. 31-Sept. 7, Kyoto, Japan, 1986, pp. 3103-3104.

[9] M. Unser, A. Steven and B. Trus, "Odd men out: a quantitative objective procedure for identifying anomalous members of a set of noisy images of ostensibly identical specimens", *Ultramicroscopy*, Vol. 19, 1986, pp. 337-347.

[10] M. Unser, M. Eden and B.L. Trus, "Unwarping of slightly distorted periodic structures using bidimensional polynomial representations", *Signal Process.*, Vol. 12, 1987, pp. 83-91.

[11] M. Unser, B.L. Trus and A.C. Steven, "A new resolution criterion based on spectral signal-to-noise ratios", *Ultramicroscopy*, Vol. 23, 1987, pp. 39-52.

[12] P. Van Wie and M. Stein, "A Landsat digital image rectification system", *IEEE Trans. Geosci. Electron.*, Vol. 15, 1977, pp. 130-137.

[13] P. Volet and M. Kunt, "Synthesis of natural structured textures", in: I.T. Young et al., eds., *Signal Processing III. Theory and Applications* (Proc. 3rd European Signal Processing Conf., The Hague, The Netherlands, 2-5 September 1986), Elsevier, Amsterdam, 1986, pp. 913-916.